In vivo processing and antibiotic activity of microcin B17 analogs with varying ring content and altered bisheterocyclic sites

Ranabir Sinha Roy, Neil L Kelleher, Jill C Milne and Christopher T Walsh

Background: The *Escherichia coli* peptide antibiotic microcin B17 (MccB17) contains four oxazole and four thiazole rings, and inhibits DNA gyrase. The role of individual and tandem pairs of heterocycles in bioactivity has not been determined previously.

Results: The two tandem 4,2-bisheterocycles in MccB17 were varied by expression of MccB17 or mutants containing altered sequences at Gly39–Ser40–Cys41 or Gly54–Cys55–Ser56. A mixture of five–nine-ring MccB17 isoforms were separated and quantitated for antibiotic potency. Mutagenesis of the thiazole–oxazole pair significantly affected antibiotic activity compared with the upstream oxazole–thiazole, which might stabilize partially cyclized intermediates against proteolysis.

Conclusions: Enzymatic heterocyclization in native MccB17 occurs distributively. Antibiotic activity correlates with the number of rings and is differentially sensitive to both the location and the identity of the 4,2-tandem heterocycle pairs in MccB17. Such tandem heterocycles might be useful pharmacophores in combinatorial libraries.

Address: Department of Biological Chemistry and Molecular Pharmacology, Harvard Medical School, Boston, MA 02115, USA.

Correspondence: Christopher T Walsh
E-mail: walsh@walsh.med.harvard.edu

Key words: antibiotic, gyrase, heterocycles, microcin B17, mutagenesis

Received: **18 January 1999**
Revisions requested: **5 February 1999**
Revisions received: **17 February 1999**
Accepted: **23 February 1999**

Published: **19 April 1999**

Chemistry & Biology May 1999, **6**:305–318
http://biomednet.com/elecref/1074552100600305

 ISSN 1074-5521

Introduction

The microcin B17 (MccB17) operon, which is present in certain strains of *Escherichia coli*, is turned on in stationary phase and encodes seven genes (*mcbABCDEFG*) that are responsible for microcin synthesis, export and immunity [1,2]. McbA, the first gene product, is a 69-amino-acid MccB17 precursor [3,4], that is subject to post-translational modification by the three-subunit McbB,C,D enzyme complex [5]. The latter converts two Gly–Ser, two Gly–Cys, a Gly–Ser–Cys and a Gly–Cys–Ser sequence in McbA (pre-proMccB17) into two oxazole rings, two thiazole rings, a 4,2-fused oxazole–thiazole ring and a 4,2-fused thiazole–oxazole ring, respectively [6,7]. The first 26 residues of this heterocyclic intermediate (proMccB17) are subsequently removed to yield mature MccB17 (Figure 1), which is exported out of the cell by a dedicated membrane-associated ATP-binding cassette transporter comprised of McbE and McbF gene products [8]. Microcin B17 arrests DNA replication in sensitive *E. coli* [9]. Self-immunity is conferred on MccB17-producing cells by the seventh gene of the operon, *mcbG*, by an as yet undetermined mechanism [8].

We previously overexpressed and purified the McbB,C,D enzyme complex (microcin B17 synthetase) [5], and have investigated the *in vitro* heterocyclization of serine and cysteine residues in both full-length McbA and minimal substrate fragments (e.g. $McbA_{1-46}$). The ATP-dependent cyclodehydration and dehydrogenation activities of the enzyme have been assayed as it processes the $McbA_{1-46}$ fragment containing the first bisheterocyclization site (Gly39–Ser40–Cys41, in the numbering scheme of McbA; Figure 1) [10]. Similar *in vitro* studies have illuminated the role of $McbA_{1-26}$ as an amphipathic helical propeptide [11], that is recognized with high affinity by the synthetase [12]. Structure–activity relationship analyses of $McbA_{1-46}$ analogs have studied the regioselectivity and chemoselectivity of bisheterocyclization [13,14], and the stoichiometry of coupled ATP cleavage (five ATP molecules hydrolyzed per heterocycle formed, under a defined set of conditions) [15]. Furthermore, the facile expression and purification of $McbA_{1-46}$ homologs fused to maltose-binding protein has allowed the demonstration that MccB17 synthetase can accept 'non-native' Gly–Cys–Cys and Gly–Ser–Ser sequences *in vitro* to generate tandem 4,2-fused bisthiazole and bisoxazole heterocycles, respectively [13].

Genetic evidence suggests that MccB17 targets bacterial DNA gyrase [16]. This enzyme catalyzes both the negative supercoiling and the relaxation of DNA that are essential for DNA replication [17]. Sensitive cells exposed to MccB17 undergo immediate cessation of DNA synthesis followed by induction of the SOS response, indiscriminate double-strand cleavage of DNA and cell death [9]. MccB17 appears to interfere with the strand nicking–religation activity of gyrase by trapping a covalent protein–DNA intermediate [16]; this is analogous to the inhibition of bacterial type II DNA topoisomerases by antibiotics such as the quinolones [18]. The eight oxazole and thiazole moieties in MccB17 are presumed to play a critical role in this process, because the rest of the molecule

Figure 1

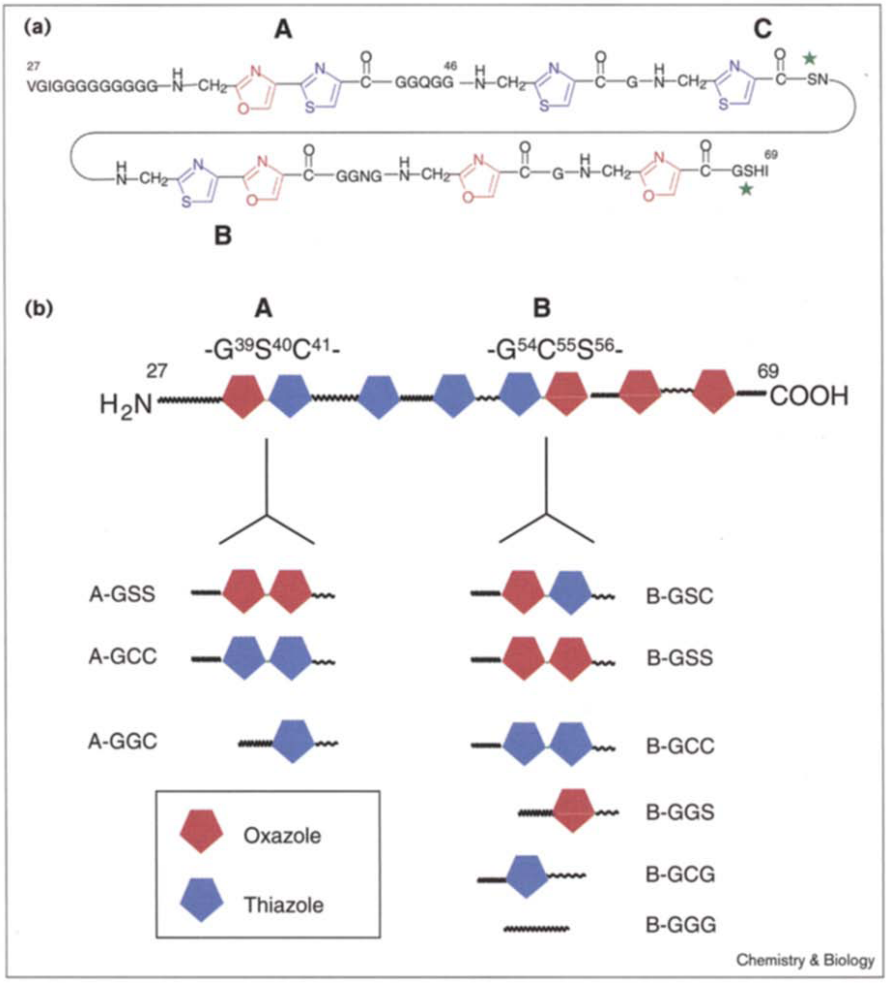

Structure of MccB17 and its analogs. **(a)** Of the three potential bisheterocyclic sites (A–C) present in the McbA precursor, only the A-site and B-site are processed to the 4,2-tandem heterocycles in mature MccB17. Two serines remain uncyclized (green stars), including Ser52 at the C-site. **(b)** The library of MccB17 analogs generated in this study, containing altered heterocycles at the A-site or B-site.

essentially constitutes a polyglycine tether. Significantly, a 4,2-fused bisthiazole moiety in the DNA-directed antitumor drug bleomycin is known to intercalate DNA [19] or to bind in the minor groove [20]; this suggests that similar roles could be played by the two tandem bisheterocycles in MccB17. We have constructed mutants at both bisheterocyclization sites of full-length McbA (Figure 1b), expressed them *in vivo* in the context of the complete MccB17 operon, isolated the product microcins and characterized them by mass spectrometry for ring content. We also report on the antibiotic activity of the altered microcins against the susceptible *E. coli* strain ZK4.

Results

Construction of mutant McbA genes

In vitro assays of $McbA_{1–46}$ fragments with purified synthetase have demonstrated that serine and cysteine permutations of the Gly39–Ser40–Cys41 sequence (the 'A'-site, A-GSC) can generally be converted to the corresponding mono/bisheterocycles [13]. An exception was the reverse regioisomer (A-GCS), which yielded only the monothiazole product. Nevertheless, the ability to generate alternative bisheterocycles in $McbA_{1–46}$ prompted us to extend this strategy to full-length McbA so that the effects on antibiotic activity could be evaluated.

As noted previously with the $mcbA_{1–46}$ gene fragment [10], codon degeneracy and consequent mispriming in the polyglycine-linker-coding region hampered mutagenesis at the downstream A-site. Three mutant *mcbA* genes with altered A-site residues were eventually obtained using splicing-by-overlap extension polymerase chain reaction (SOE–PCR) [21] and unique site elimination (USE) [22] mutagenesis strategies. Together with the B-site mutants constructed by the same methods, a library of genes encoding full-length McbA with altered bisheterocycles (A-GSS, A-GCC, B-GSC, B-GSS and B-GCC), single ring deletions (A-GGC, B-GCG and B-GGS), and a bisheterocycle 'knockout' (B-GGG) was created (Figure 1b). To maximize the yield of mutant microcins, these genes were expressed in the context of the entire *mccB17* operon cloned into the high-copy vector, pUC19 (pUC19–*mccB17*) [15].

Microcin B17 is a mixture of heterocyclic polypeptides

The wild-type and mutant MccB17 antibiotics were expressed in *E. coli* strain DH5α. Given that microcin production is stimulated by limiting nutrients [23], cultures were grown to stationary phase in minimal media prior to harvesting. For each preparation (including wild-type MccB17), several products with slightly shorter retention times than that of the authentic microcin were also obtained in the high-performance liquid chromatography (HPLC) purification (Figures 2a and 3a). As illustrated in Figures 2b and 3b for wild-type MccB17 and the A-GCC mutant, respectively, analysis of these HPLC fractions by matrix-assisted laser desorption ionization–time of flight mass spectrometry (MALDI–TOF MS) or electrospray ionization–Fourier transform (ESI-FT)–MS identified the peptides to be partially cyclized microcins containing 1–3 heterocycles less than the expected complement of rings (each oxazole or thiazole ring formed is accompanied by a mass decrease of 20.03 Da due to the loss of water and two hydrogen atoms). The deficit (Δ) in heterocycle content is hereafter included in the annotation of these peptides (Δ^{-1}, Δ^{-2} and so on) to distinguish them from the fully heterocyclized 'native' (Δ^0) isoform.

As previously noted for *in vitro* assays of the $McbA_{1-46}$ fragment [13], the observation of partially cyclized intermediates implies that the *in vivo* heterocyclization of full-length McbA is distributive rather than processive, with repetitive dissociation and rebinding of partially cyclized intermediates. The resulting sample heterogeneity necessitates rigorous HPLC purification of each microcin product, and confirmation of ring content by mass spectrometry, so that comparative assays of bioefficacy are performed with antibiotics containing the full complement of heterocycles. Typically, 3.5 mg of pure Δ^0 microcin was obtained in >90% purity from 1l of culture. The yield was lower (<1 mg/l culture) for microcins containing monooxale or bisoxazole moieties at either bisheterocyclization site. The processing of additional serine residues in these mutants (A-GSS, B-GSS and B-GGS) probably introduced kinetic traps during heterocyclization, which decreased the yield of mature antibiotic. In support of this hypothesis, *in vitro* chemoselectivity studies of $McbA_{1-46}$ have shown that oxazole rings are formed at least 100-fold slower than thiazole rings [13].

Figure 2

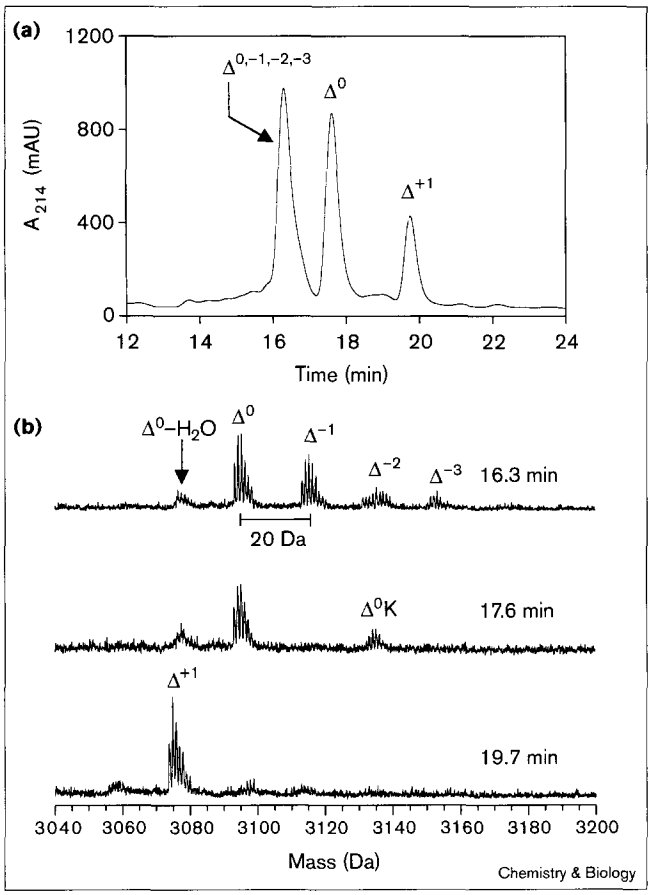

Purification and characterization of wild-type MccB17. **(a)** HPLC trace of crude MccB17 injected on a Vydac C_{18} preparative reversed-phase column. Partially cyclized isoforms containing five–seven rings ($\Delta^{-3,-2,-1}$) and a nine-ring (Δ^{+1}) MccB17 eluted with different retention times, in addition to the native eight-ring (Δ^0) antibiotic. In this figure mAU stands for milli-absorbance units. **(b)** MALDI–TOF MS analysis of the HPLC fractions eluting at 16.3, 17.6 and 19.7 min, corresponding to the three peaks in Figure 2a. The following MccB17 $[MH]^+$ isoforms were detected: nine-ring (Δ^{+1}, M_{obs} = 3073.9 Da, M_{calc} = 3073.0 Da), eight-ring (Δ^0, M_{obs} = 3094.2 Da, M_{calc} = 3094.0 Da), seven-ring (Δ^{-1}, M_{obs} = 3114.4 Da, M_{calc} = 3114.1 Da), six-ring (Δ^{-2}, M_{obs} = 3133.5 Da, M_{calc} = 3134.1 Da) and five-ring (Δ^{-3}, M_{obs} = 3152.0 Da, M_{calc} = 3154.1 Da). Molecular ions resulting from the potassium adduct (Δ^0K) and from the loss of water (Δ^0-H_2O) are also indicated for the eight-ring isoform.

Discovery of a ninth heterocycle in MccB17

Intriguingly, in the HPLC purification of wild-type MccB17 and certain mutants, a minor component (~16% of the total extract) eluting after the authentic microcin was observed to contain an extra ring, as indicated by an additional mass deficit of 20 Da relative to the Δ^0 species in the mass spectrum, and confirmed by subsequent mass spectrometry (MS/MS) analysis (see below). For example, the observed molecular weight (M_{obs}) of native MccB17 (eluting at 17.6 min during HPLC purification; Figure 2a) was measured by MALDI–TOF MS to be 3093.2 Da (M_{calc} = 3093.0 Da), thus verifying its eight-ring composition (Figure 2b). In comparison, the relative molecular weight (M_r) of material eluting at a later retention time (19.7 min) was 3072.9 Da, consistent with the formation of a ninth ring in this material (M_{calc} = 3073.0 Da). Similarly, a nine-ring isoform of the B-GSC mutant, an eight-ring B-GGS and a seven-ring B-GGG microcin, each containing an extra heterocycle compared with the Δ^0 product, were also isolated. In keeping with the nomenclature described earlier, these derivatives are hereafter referred to as the Δ^{+1} microcins.

Figure 3

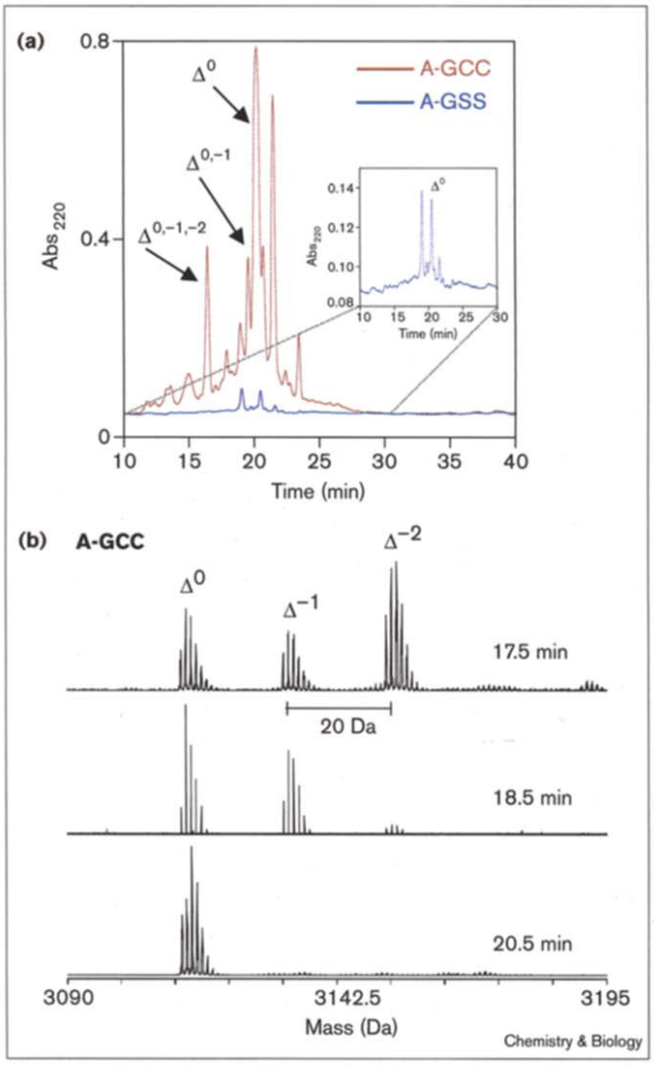

Purification and characterization of the A-GCC and A-GSS MccB17 analogs. **(a)** HPLC traces of the crude microcins. Extracts from 300 ml of producer cells were purified by HPLC as described in the Materials and methods section. The low expression of A-GSS (blue, inset) relative to A-GCC (red) is evident, as is the presence of multiple isoforms. **(b)** ESI–FT spectra acquired at 9.4 Tesla for three HPLC fractions collected during the purification of A-GCC. Retention times are indicated alongside each mass spectrum. Eight-ring (Δ^0, M_{obs} = 3109.00 Da, M_{calc} = 3109.03 Da), seven-ring (Δ^{-1}, M_{obs} = 3129.03 Da, M_{calc} = 3129.08 Da) and six-ring (Δ^{-2}, M_{obs} = 3149.06 Da, M_{calc} = 3149.12 Da) isoforms were detected as shown. The nine-ring Δ^{+1} isoform was not observed for this MccB17 mutant.

The nine-ring (Δ^{+1}) MccB17 contains three 4,2-linked bisheterocycles

Two serine residues (Ser52 and Ser67) remain unprocessed in the mature eight-ring MccB17 antibiotic (Figure 1). Isolation of a nine-ring Δ^{+1} microcin during the purification of MccB17 therefore, prompted detailed MS/MS analysis of this molecule to determine which serine residue was cyclized to the extra oxazole ring. To localize the position of the ninth heterocycle, triply-charged ions of Δ^{+1} MccB17 obtained by electrospray ionization were subjected to MS/MS using collisionally activated dissociation (CAD) [24]. We have utilized this technique previously to characterize heterocycle formation in $McbA_{1-46}$ fragments [14]. Such low-energy CAD results in the cleavage of different amide bonds within the polypeptide ions, each of which produces corresponding amino-terminal ('b') and carboxy-terminal ('y') fragments [25]. A comparison of the M_r values of these fragments (20.03 Da deficit per heterocycle formed) with those calculated for the corresponding uncyclized fragments allows the position of heterocycles to be determined within the primary sequence.

The MS/MS spectrum of Δ^{+1} MccB17 (Figure 4a) yielded 15 fragment ions (in addition to several neutral-loss peaks). Of these ions, six could be identified as comprising the b-ion series, b_6–b_{11} (corresponding to 6–11-mer sequences from the amino terminus; Figure 4b). An additional six fragment ions corresponded to heterocycle-containing sequences at the carboxyl terminus (y-ions; Figure 4b). The three remaining ions could not be assigned to any particular fragment resulting from one or two amide-bond cleavages. Diagnostic data were obtained from the y-type ions, which encompass the residues that are heterocyclized in MccB17. For example, the y_9 and y_{10} fragment ions had M_r values corresponding (within error) to those of their counterparts in the MS/MS spectrum of Δ^0 MccB17 (40.04 and 40.02 Da lower than the values predicted for the uncyclized y-ion fragments, respectively). These data indicate that the carboxy-terminal ten residues in Δ^{+1} MccB17 contain only two heterocycles (as in the native Δ^0 microcin). Corroborating this result, the y_{16} ion at ~1210 *m/z* (Figure 4a) reveals that the carboxy-terminal 16 residues of Δ^{+1} MccB17 are identical to those in the Δ^0 isoform, and contain four rings (denoted $^{4r}y_{16}$). Both observations discount the residue Ser67 as being the source of the ninth heterocycle. Lastly, ions corresponding to $^{6r}y_{20}$ and $^{7r}y_{25}$ were observed, indicating that the carboxy-terminal 20 and 25 residues, predicted to contain only five and six cyclization sites, respectively, actually contained an additional cyclized residue each. Taken together, the y-type fragment ions indicate that the additional ring is located predominantly (>90%) between residues Gly50 and Asn53, which is consistent with cyclization of Ser52 (and not Ser67) to an oxazole ring.

UV spectroscopy of mutant microcins

To date, the antibiotic activity of MccB17 has been determined by the critical dilution method [26], with one unit defined as the amount of microcin present in a 10 µl sample of the highest dilution able to produce a clear zone (or halo) of growth inhibition on a lawn of sensitive cells [9]. Unfortunately, this method is subject to considerable error, and it is preferable to correlate microcin activity with the actual amount of antibiotic present in the assay. Given that dry weights of submilligram-to-milligram quantities of microcins

Figure 4

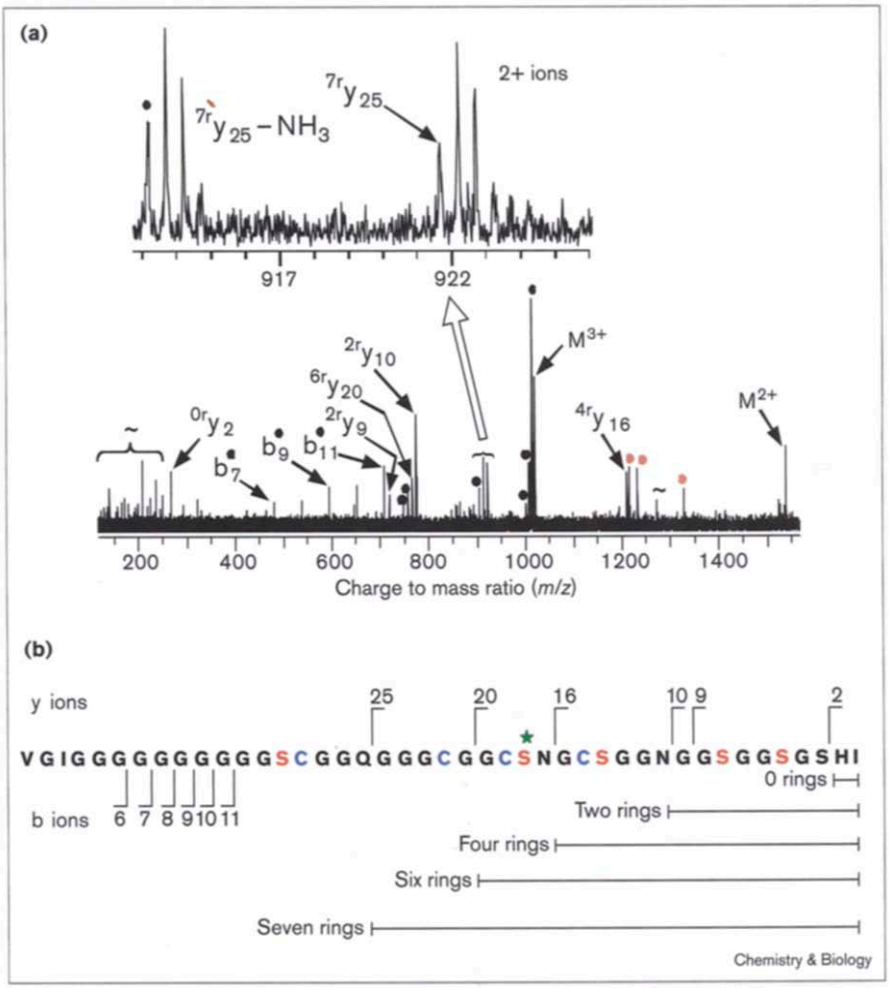

MS/MS analysis of the nine-ring (Δ^{+1}) MccB17 isoform. **(a)** Full MS/MS spectrum acquired on a 4.7 Tesla ESI-FT MS, showing several b-type and y-type fragment ions produced by collisionally activated dissociation (CAD). Neutral loss peaks (due to water or ammonia loss) are indicated by black dots. Three ions (red dots) could not be assigned to fragments resulting from single or double amide bond cleavages. The A+1 isotopic peaks for 1^+ fragment ions in the low *m/z* section of the spectrum (< 250 *m/z*) were absent. Hence, these fragment ions could not be distinguished from frequency spikes ('~'). Also shown is an expansion of the spectrum corresponding to the diagnostic 2+ $^{7r}y25$ fragment ion (M_{obs} = 1841.5 Da, M_{calc} = 1841.4 Da). **(b)** Schematic, summarizing the various amino-terminal ('b') and carboxy-terminal ('y') fragment ions observed during CAD of Δ^{+1} MccB17. The heterocycle content of each y-ion (inferred from its molecular mass) is also shown. Cyclization of Ser52 (green star) results in the formation of $^{6r}y_{20}$ and $^{7r}y_{25}$ fragment ions, each containing an extra ring compared to the corresponding fragments from native eight-ring MccB17.

are generally unreliable, the UV properties of oxazole and thiazole moieties were exploited to estimate microcin concentration, which was expressed in 'normalized absorbance units' (NAUs). We have previously demonstrated that both monoheterocycles and bisheterocycles in MccB17 absorb at 240–254 nm, with the latter also absorbing at 280 nm because of extended ring conjugation [13]. The NAU of a microcin solution was calculated as NAU = A_{254}/N, where A_{254} is the absorbance of the solution at 254 nm, and N is the number of heterocycles in the microcin (N = 8 for Δ^0 MccB17; Table 1). For the diverse microcin analogs generated in this study, stock solutions of pure antibiotic ranging from 0.6-4.0 NAU were obtained. Quantitative amino-acid analyses (QAA) of these solutions were conducted in parallel, which enabled the NAU values to be correlated with the actual antibiotic concentrations. These conversion factors (summarized in Table 1) enabled spectroscopic determination of microcin concentrations in subsequent purifications, typically with <15% error (as determined by QAA). In addition, a stock solution of purified Δ^0 MccB17 of defined concentration was assayed by the critical dilution method, and it was determined that one unit of activity (as defined by the latter) corresponds to ~18.5 ng of MccB17.

Antibiotic activity of the nine-ring (Δ^{+1}) MccB17 derivative

Bisheterocyclization of the Gly50–Cys51–Ser52 sequence (hereafter referred to as the 'C'-site of McbA; Figure 1) in Δ^{+1} MccB17, and presumably in the Δ^{+1} MccB17 mutants, results in a molecule containing three tandem 4,2-fused bisheterocycles. Given that these moieties have been identified as probable partners for interaction with DNA, we anticipated an altered bioactivity for the nine-ring (Δ^{+1}) MccB17 compared with the native eight-ring isoform. Activity comparisons were obtained using the bioassay developed by Yorgey [27], with some modifications. Defined amounts of microcin (up to 1.6 µg) were spotted in 2 µl aliquots on lawns of MccB17-sensitive *E. coli* ZK4 cells [6], which were then incubated for 12 h at 37°C. Antibiotic activity resulted in cell death and consequent halos of growth inhibition on the lawn (Figure 5a). Densitometric analysis of these halos was subsequently used to construct activity curves for each antibiotic (Figure 5b).

Table 1

Quantification of microcin concentration by UV spectroscopy and quantitative amino acid analysis (QAA).

MccB17 analog	Number of rings (N)	Concentration of Microcin /NAU (μM NAU^{-1})
Wild-type MccB17	8	204
A-GSS	8	220
A-GCC	8	190
B-GSC	8	277
B-GSS	8	183
B-GCC	8	334
B-GGS	7	226
B-GCG	7	237
B-GGG	6	193

Concentration was initially expressed in normalized absorbance units (NAU) based on the absorbance at 254 nm and the number of rings (N) present in the MccB17 analog, as defined in the Results section. The QAA of the stock solutions enabled subsequent spectroscopic measurements to be converted to SI units (μM) using the listed conversion factors.

An increase in microcin concentration was accompanied by a corresponding increase in the death of sensitive ZK4 cells. Limited diffusion of the antibiotics through the agar media led to saturation of activity (quantified as halo size and intensity) at high microcin concentrations. It is reasonable to assume that the different microcins exhibit similar extents of diffusion, because aliquots of constant volume (2 μl) were spotted on each lawn. The differences in growth inhibition observed at saturation, therefore, parallel the relative efficacies of the various microcin analogs. It is evident from the activity curves presented in Figure 5b that the Δ^{+1} MccB17 isoform exhibits ~40% higher activity against sensitive *E. coli* ZK4 cells, compared with the native eight-ring (Δ^0) antibiotic. Consistent with this observation, the activities of other competent Δ^{+1} MccB17 analogs were also higher than those of the corresponding Δ^0 products (see below). The potency of a particular MccB17 analog therefore correlates with the number of bisheterocycles present in the microcin.

Mutagenesis of the A-site (Gly39–Ser40–Cys41) in MccB17

The tandem 4,2-fused oxazole–thiazole moiety at the A-site of native MccB17 (A-GSC) might interact with target DNA (for example in a ternary DNA–gyrase–microcin complex). We therefore constructed a single-ring mutant at this site (A-GGC) to investigate whether loss of the bisheterocycle affected bioactivity. Two double mutants (A-GCC and A-GSS) that would contain the bisthiazole moiety found in the antitumor drug bleomycin A [28] and the bisoxazole fragment of the antiviral agent hennoxazole A [29], respectively, were also prepared. The *in vitro* bisheterocyclization of these sequences in $McbA_{1-46}$ has been previously demonstrated [13], and their incorporation in full-length McbA allowed the opportunity to evaluate the bioactivity of microcins with non-native bisheterocycles. The reverse regioisomer (A-GCS) was not investigated, because the *in vitro* studies had shown that the synthetase cannot process this sequence to completion.

Figure 5

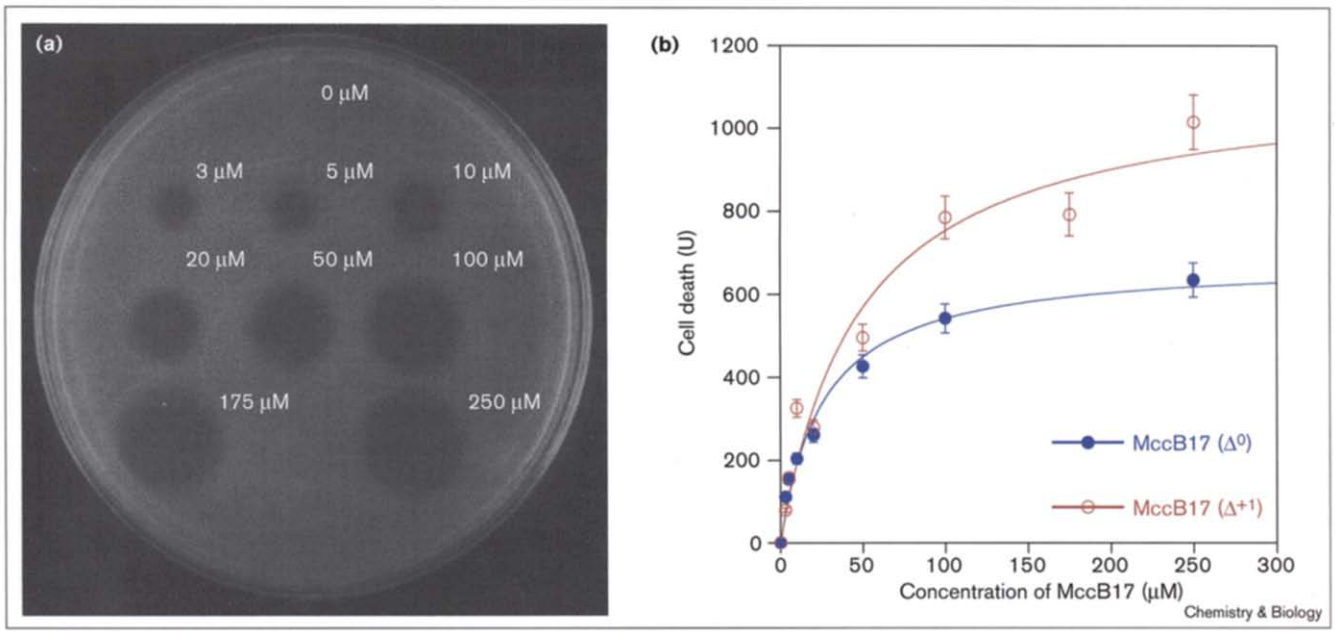

Bioassay of eight-ring and nine-ring MccB17s. **(a)** Halos of growth inhibition obtained upon titration of eight-ring (Δ^0) MccB17 on a lawn of sensitive *E. coli* ZK4 cells. The concentration of antibiotic that produced each halo is listed. **(b)** Activity curves for the Δ^0 and Δ^{+1} isoforms of MccB17 obtained by densitometric integration of halos of growth inhibition of ZK4 cells. Cell death is reported in arbitrary units (U).

As with native MccB17, partially cyclized intermediates were observed during the HPLC purification of A-GCC (Figure 3a). Both, seven-ring (Δ^{-1}) and six-ring (Δ^{-2}) species in addition to native (Δ^0) A-GCC microcin were detected in the ESI-FT MS spectra of the HPLC fractions (Figure 3b). The net yield of mutant A-GCC microcin was comparable to that of wild-type MccB17, although very low quantities of the A-GSS mutant were obtained from cell cultures. This result is consistent with our prior observations that the *in vitro* processing of A-GSS (in the context of $McbA_{1-46}$) proceeds very sluggishly (~5% conversion in 24 h) [13], and that the chemoselectivity of synthetase-mediated heterocyclization favors the processing of cysteine residues relative to serine residues [13,14]. The low abundance of microcin-related peptides in the expression of A-GSS indicated that microcin production was severely impaired upon incorporation of the tandem serines at the A-site, which suggests that the cyclization of downstream heterocycles might occur only after bisheterocyclization at the A-site. If so, the A-GSS mutant sequence in full-length McbA probably acts as an upstream kinetic trap and impedes the processing of subsequent residues.

The activity plots for the Δ^0 A-site mutant microcins are presented for comparison with that of Δ^0 MccB17 in Figure 6. Substitution of the A-site oxazole–thiazole moiety in native MccB17 with a bisthiazole ring (A-GCC) did not significantly affect antibiotic activity, although the bisoxazole analog (A-GSS) exhibited only 70% efficacy. Hence, the composition of each individual ring within a bisheterocycle (oxazole versus thiazole) can influence microcin activity. The single-ring A-GGC analog was the only construct for which no microcin production could be detected *in vivo*. HPLC and MS analyses of the extract failed to reveal any McbA-related products (data not shown), even though the fidelity of the expression vector was verified by oligonucleotide sequencing. In addition, no bioactivity could be detected in bioassays of the crude cell extracts. An alternative *in vitro* strategy to obtain the A-GGC mutant was subsequently developed to circumvent these difficulties in antibiotic production.

In vitro construction of the A-GGC MccB17 analog

Single thiazole rings have been efficiently introduced into the A-site of $McbA_{1-46}$ by *in vitro* incubation of analogs containing Gly–Cys sequences (A-GGC and A-GCG) with purified synthetase [13]. This *in vitro* strategy was therefore extended to full-length McbA to construct the A-GGC microcin analog. The mutant A-GGC McbA polypeptide was separately expressed and affinity-purified using an amino-terminal His_6 tag (Figure 7a). Upon incubation with affinity-purified MccB17 synthetase [10] for 25 h, the fully processed A-GGC (Δ^0) promicrocin containing seven heterocycles was obtained (in addition to partially cyclized intermediates). Digestion of this mixture with chymotrypsin

Figure 6

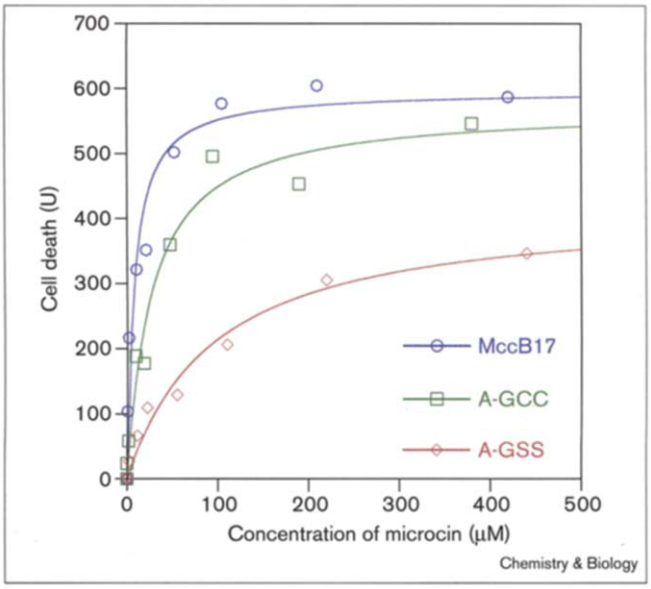

Activity curves for the Δ^0 isoforms of wild-type MccB17 and the A-site analogs.

enabled the removal of virtually the entire propeptide sequence by cleavage at the Leu25–Gly26 amide bond. The mature antibiotic ('α-GGC') comprised of residues 26–69 of the McbA polypeptide was purified by HPLC and its identity was confirmed by MALDI-TOF MS (M_{obs} = 3141.4 Da, M_{calc} = 3140.0 Da). The additional residue (Gly26) retained at the amino terminus after proteolytic removal of the propeptide does not significantly interfere with microcin activity, as shown by the measurable bioactivity of wild-type MccB17 ('α-WT'; Figure 7b) produced by this route. Although titration experiments were prevented by the limited amounts of each microcin synthesized *in vitro*, both α-WT and α-GGC did produce zones of growth inhibition on a lawn of sensitive ZK4 cells (Figure 7b).

Mutagenesis of the B-site (Gly54–Cys55–Ser56) in MccB17

Unlike the A-site, which has been the focus of extensive *in vitro* analysis, the B-site thiazole–oxazole moiety of MccB17 has remained outside the scope of systematic mutagenesis studies because the appropriate substrates are large and difficult to evaluate (the B-site comprises the fifth and sixth residues to be cyclized out of eight). We elected to express and test all possible combinations of B-site bisheterocycles (B-GSC, B-GSS, and B-GCC) in the context of full-length McbA, in addition to single-ring deletions (B-GCG and B-GGS) and the bisheterocycle knockout (B-GGG).

The increased importance of the native B-GCS bisheterocycle to microcin activity (relative to the A-site) was immediately apparent in bioassays with the B-site mutants. Microcin activity was adversely affected by even

Figure 7

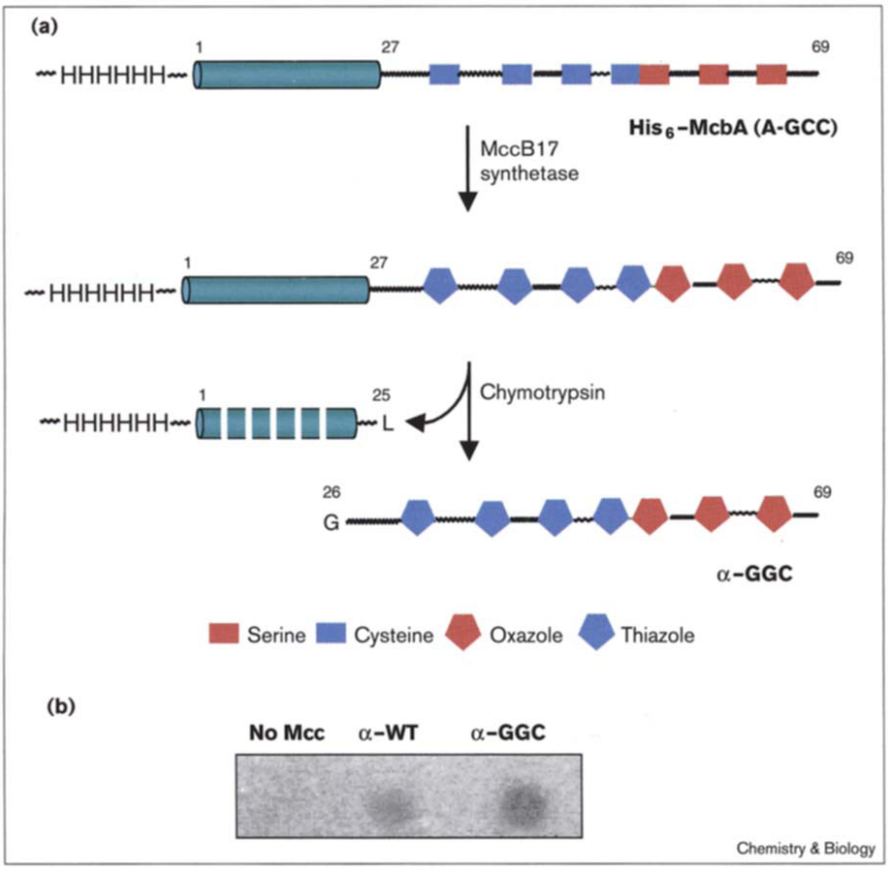

In vitro synthesis of α-GGC. **(a)** The mutant A-GGC His_6–McbA fusion peptide was heterocyclized by incubation with affinity-purified MccB17 synthetase. Subsequent treatment with chymotrypsin released most of the propeptide sequence ($McbA_{1-25}$), with a single glycine residue retained at the amino terminus (the protease also cleaves five other upstream sites within the propeptide). The fully processed (seven-ring) product (α-GGC) encompasses residues 26–69 of McbA, and was purified from partially cyclized intermediates by HPLC. Native (eight-ring) MccB17 was also obtained from wild-type McbA by this route. **(b)** Zones of growth inhibition on lawns of sensitive *E. coli* ZK4 cells treated with the microcins generated *in vitro*. Cells were grown unperturbed (no Mcc), or treated with 'wild type' MccB17 (α-WT) or the A-site monothiazole analog (α-GGC). The results are strictly qualitative, given that the limited amounts of microcin generated *in vitro* prevented the measurement of antibiotic concentrations in these assays.

the slightest alteration in bisheterocycle composition or content at the B-site. Thus, each altered bisheterocycle (B-GCC, B-GSS, and even the reverse regioisomer B-GSC, which mimics the A-site) exhibited less than 30% activity relative to wild-type MccB17 (Figure 8). In turn, the B-site bisheterocycle mutants were typically 50–60% more active than analogs containing only a single oxazole or thiazole ring at this site (B-GCG and B-GGS). As with wild-type MccB17, the Δ^{+1} B-site mutant microcins exhibited 2–5-fold increased bioactivity relative to the corresponding Δ^0 antibiotic. Notable exceptions were the Δ^{+1} and Δ^0 derivatives of the B-site knockout (B-GGG), both of which were completely inactive within the sensitivity limits of the bioassay, wherein 0.3% of the bioactivity of the most potent microcin (Δ^{+1} MccB17) could have been detected.

Investigation of antibiotic uptake in microcin-sensitive cells

Although the structure–activity studies of the A-site and B-site analogs described in this work implicate the bisheterocycle moieties as key determinants in the bioactivity of MccB17, the poor efficacies of mutant microcins depicted in Figure 8 could simply have resulted from a selectively decreased uptake of the altered antibiotics by sensitive cells. To evaluate this possibility, a bioassay that normalizes for antibiotic uptake was utilized as the second probe for microcin activity. Cell membranes were first permeabilized by treatment with toluene, which allows the free passage of small molecules (including microcins) into the cell. Replicative DNA synthesis was subsequently assayed *in vivo* using a modified assay originally developed by Moses [30], which measures the incorporation of labeled [α-^{32}P]dTTP into genomic DNA. Given that the antibiotic stalls DNA synthesis, lower rates of nucleotide incorporation would be anticipated in the presence of exogenous microcins. A comparison of these rates with the bioassay data for the mutant microcins depicted in Figure 8 reveals whether or not bisheterocycle moieties were important for antibiotic uptake by transport proteins in nonpermeabilized cells.

The rates of replicative DNA synthesis in toluene-permeabilized *E. coli* ZK4 cells that were exposed to wild-type Δ^0 MccB17 and various Δ^0 B-site mutants are presented in Figure 9. The microcin concentration in these assays (125 μM) produced at least 95% of the antibiotic activity observed at saturation in the corresponding lawn bioassays (Figure 8) and was high enough to detect even low levels of inhibition of DNA synthesis. All four deoxynucleotide triphosphates were included in the assay, in addition to magnesium ions, potassium ions and ATP. Under these conditions, wild-type Δ^0 MccB17 completely

Figure 8

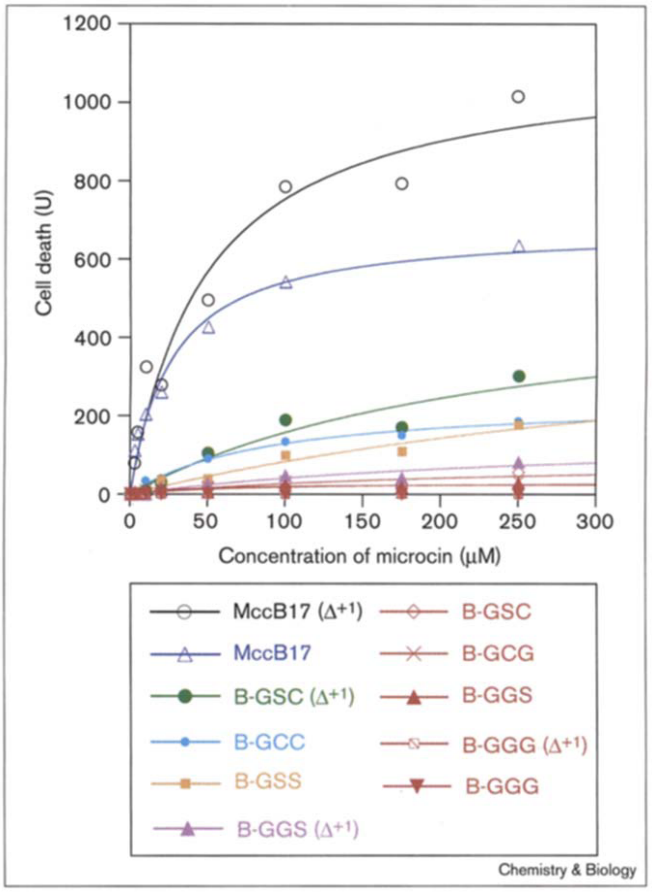

Activity curves for Δ^{+1} and Δ^{0} isoforms of wild-type MccB17 and the various B-site analogs.

Figure 9

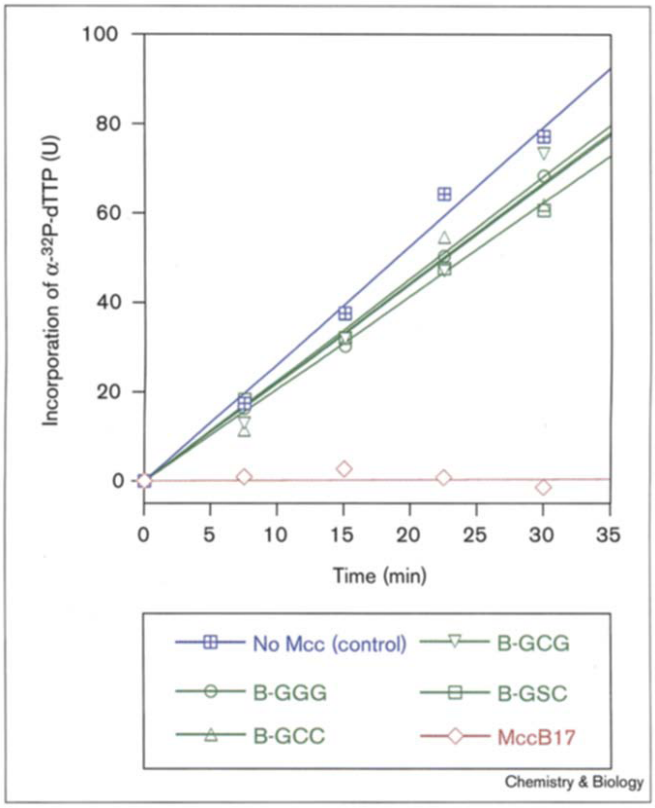

Inhibition of replicative DNA synthesis in ZK4 cells treated with MccB17 or different B-site mutants. Rates of *in vivo* DNA synthesis were obtained by measuring the incorporation of radiolabeled dTTP in toluene-permeabilized ZK4 cells (no Mcc), and in similar cells exposed to 150 μM antibiotic.

abolished DNA replication as indicated by the absence of radiolabel in trichloroacetic acid (TCA)-precipitates of the genomic material. In comparison, control cells that were not exposed to antibiotic exhibited time-dependent incorporation of [α-^{32}P]dTTP (Figure 9), which is consistent with *in vivo* semiconservative DNA synthesis under the assay conditions [30].

Four mutant microcins (B-GGG, B-GCC, B-GCG, and B-GSC) that span the spectrum of bioactivity observed with the B-site analogs were assayed for their effects on *in vivo* DNA synthesis. Significantly, these microcins continued to exhibit low levels of bioactivity despite free diffusion of the antibiotics into the sensitive cells (~16% inhibition of DNA synthesis, which is barely significant, given the limited sensitivity of the assay). The observed differences in bioefficacy between the mutant microcins (3–4%) is within the experimental error of the assay (~11%). The data confirm that the poor bioefficacy of the mutant microcins is not due to limited uptake of the altered antibiotics by the sensitive cells, but results from impaired interactions of the drugs with their target.

To further investigate the sensitivity of replicative DNA synthesis to exogenous microcin, the assays that had been conducted at a fixed concentration of antibiotic were repeated over a range of concentrations for native (Δ^{0}) MccB17 and the corresponding B-GCC (bisthiazole) analog. As illustrated in Figure 10, the titration of native MccB17 into permeabilized *E. coli* ZK4 cells gave a linear dose-response for inhibition of DNA replication (IC_{50} ~64 μM). In contrast, the inhibition of DNA replication by B-GCC could not be increased above 20% (Figure 10), even with millimolar concentrations of antibiotic (data not shown).

Bioassays of mutant microcins with MccB17-resistant *E. coli*

Genetic studies have revealed that an Arg751→Trp point mutation in the B subunit of DNA gyrase (the presumed cellular target of MccB17) confers resistance to this antibiotic [16]. The *E. coli* strain VM11 containing this mutation in *gyrB* does not show detectable growth inhibition upon exposure to high concentrations of wild-type Δ^{0} MccB17 (up to 250 μM) in a lawn bioassay similar to the one described earlier (data not shown). To investigate whether

Figure 10

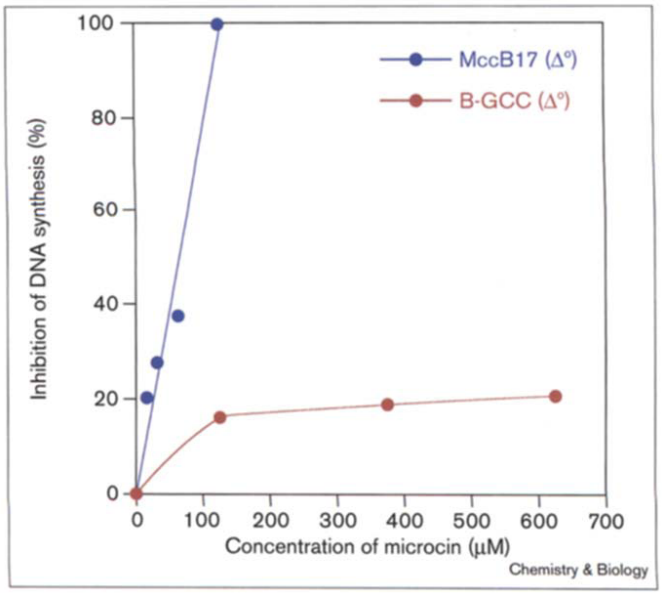

Inhibition of replicative DNA synthesis in ZK4 cells upon titration with MccB17 or B-GCC. Wild-type MccB17 completely inhibits DNA synthesis (IC_{50} ~64 μM), whereas the inhibition by B-GCC saturates at ~20%.

this resistance may have arisen from altered interactions between the native bisheterocycles in MccB17 and residues in the mutant GyrB protein (Trp751 in particular), each A-site and B-site microcin analog was bioassayed on a lawn of VM11 cells. Bioactivity of certain microcin analogs against VM11 would be anticipated if the corresponding A-site or B-site heterocycles could circumvent the protection afforded by the change at residue 751 in GyrB. As with wild-type MccB17, however, none of the mutants generated in this study (including their Δ^{+1} isoforms) exhibited bacteriocidal or bacteriostatic properties against VM11 (data not shown). Hence, the mechanism of resistance conferred by the Arg751→Trp mutation in GyrB cannot be bypassed by any of the mutations at the A-, B- and C-bisheterocyclization sites of MccB17.

Discussion

The molecular basis of interactions between oxazole and thiazole rings (present in natural products such as the antitumor agent bleomycin [28], the protein synthesis inhibitor GE2270A [31], and the antibacterial MccB17 [32]) and their diverse DNA, RNA, and protein targets is poorly understood. A particular feature to note is the frequent occurrence of tandem 4,2-linked bisheterocycles in these molecules, derived from the biosynthetic double cyclodehydration of adjacent cysteine and serine residues. In bleomycin, a 4,2-bisthiazole moiety intercalates DNA [19] and is also proposed to function as a minor-groove-binding element [20]. MccB17 has two such 4,2-tandem heterocycles in its complement of eight heterocycles: the thiazole–oxazole pair at the A-site (derived from Gly39–Ser40–Cys41) and the oxazole–thiazole reverse regioisomer at the B-site (corresponding to the Gly54–Cys55–Ser56 triad). Given that the genes for MccB17 biosynthesis (*mcbA*), post-translational heterocyclization (*mcbBCD*), export (*mcbEF*) and immunity (*mcbG*) are known, and that several attributes of the *in vitro* heterocyclization of McbA by the McbB,C,D enzyme complex are established, we have now examined the *in vivo* production and antibiotic activity of MccB17 analogs containing altered heterocycles at the A-site and B-site.

We have previously demonstrated that bisoxazoles and bisthiazoles (moieties not present in native MccB17) can be obtained from Gly39–Ser40–Ser41 (GSS) and Gly39–Cys40–Cys41 (GCC) mutant sequences introduced at the A-site of an $McbA_{1–46}$ substrate fragment by *in vitro* incubation with purified synthetase [13]. Single oxazole and thiazole rings have been similarly introduced using Gly–Ser and Gly–Cys sequences, respectively. The regioselectivity of bisheterocyclization is modulated by local sequence context, because a Gly39–Cys40–Ser41 mutant sequence in $McbA_{1–46}$ is cyclized only to the monothiazole [13], whereas the otherwise identical Gly54–Cys55–Ser56 B-site in full-length McbA is completely processed to the thiazole–oxazole. On the basis of these studies, nine full-length mutant *mcbA* genes containing glycine, cysteine and serine permutations at the A-site or B-site were engineered to alter the pairs of 4,2-tandem heterocycles in the mature antibiotic (for example to introduce a bisthiazole pair or a single thiazole ring in place of the oxazole–thiazole or thiazole–oxazole pairs).

The mutant *mcbA* genes were expressed in the context of the entire *mccB17* operon in the high-copy plasmid pUC19–*mccB17* [15], which allowed enough antibiotic product to be expressed for purification and characterization by HPLC and MS. The MS analysis was essential for determining the heterocycle content of microcin fractions separated by HPLC. A subsequent calibration of microcin concentrations by UV spectroscopy and quantitative amino-acid analysis allowed comparative analysis of antibiotic potency for each microcin species by quantifying bacterial cell-killing activity on agar plates. Densitometric integration of the zones of growth inhibition in dilution assays with lawns of sensitive *E. coli* ZK4 cells gave highly reproducible saturation curves (Figures 6 and 8) that allowed a proper comparison to be made between wild-type and various mutant MccB17 analogs. The results are summarized in Figure 11, which compares the maximum growth inhibition of ZK4 cells exposed to each antibiotic relative to the nine-ring (Δ^{+1}) MccB17.

Unanticipated results quickly emerged, even from cultures overproducing and modifying the wild-type McbA sequence: multiple isoforms corresponding to partially

Figure 11

Relative bioefficacies of the MccB17 analogs and isoforms obtained in this study. Data correspond to the maximum growth inhibition obtained on a lawn of sensitive ZK4 cells and are normalized relative to the most potent microcin (Δ^{+1} MccB17). The bisheterocycles present in Δ^{+1} and Δ^{0} MccB17 are shown schematically, and only the altered A-sites or B-sites are denoted for the mutant microcins.

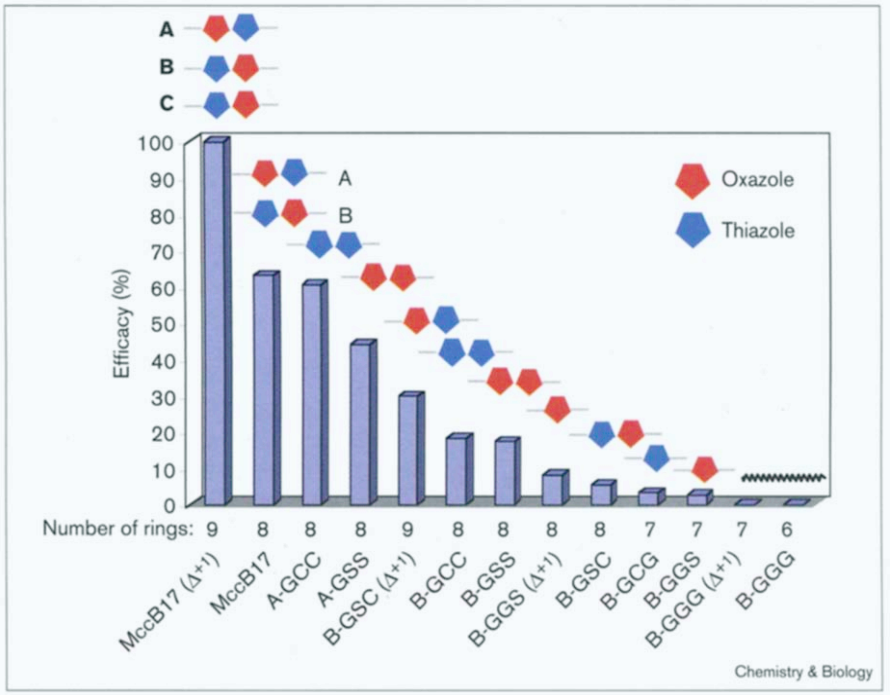

cyclized microcins were detected by HPLC and MS analyses. Similar species were also detected in the prototypic producer strain MC4100(pMM39), which carries the *mccB17* operon in the pBR322 vector (data not shown). We have observed the spontaneous precipitation of these components (and of mature MccB17 to a certain extent) in crude acid extracts upon overnight storage at 4°C, which might have prevented detection of the partially processed isoforms in prior studies [3]. Species with as few as five rings out of the normal complement of eight heterocycles in MccB17 were active as antibiotics (data not shown). These observations suggest that thiazole and oxazole ring formation occurs in discrete steps and that five-, six- and seven-ring ($\Delta^{-3,-2,-1}$) intermediates accumulate along with the eight-ring (Δ^{0}) mature MccB17.

A second unexpected result was the observation of a Δ^{+1} MccB17 isoform containing an extra ring. MS/MS analysis localized the site of this ninth ring to Ser52, which sets up a third 4,2-tandem bisheterocycle (thiazole–oxazole) in this microcin variant at the C-site (Gly50–Cys51–Ser52). It appears that introduction of the extra oxazole ring might be a peculiarity of the excess cyclodehydration capacity of McbB,C,D (for example outpacing the export capacity of McbE,F with regard to the normal eight-ring MccB17 product). Consistent with this hypothesis, no Δ^{+1} MccB17 was detected in extracts of MC4100(pMM39) cells, which contain a duplication of the genes for export (*mcbEF*) and immunity (*mcbG*) [8]. Nonetheless, a clear increase in antibiotic potency was observed in the several Δ^{+1} mutant microcins containing the new tandem bisheterocycle (30–40% higher bioefficacy relative to the corresponding Δ^{0} isoform). This result reinforces the thought that 4,2-tandem heterocycles might be DNA-targeting, antibiotic-inducing structural elements to be incorporated, for example, in the strategies for library construction of bioactive natural product mimetics.

As illustrated in Figure 11, the introduction of non-native bisheterocycle combinations at the A-site (A-GCC and A-GSS) resulted in only a modest decrease in bioefficacy (0–30%), whereas mutagenesis at the B-site had a greater impact on antibiotic activity. The results for the A-site and B-site mutants suggest distinct functions for each bisheterocycle in the mature MccB17 antibiotic. For example, the low activity of B-GCC (~25%) contrasted sharply with that of the A-GCC mutant, the latter being indistinguishable from native microcin B17. Differing potencies were also noted for A-GSS (70%) and B-GSS (17%). In addition, whereas the B-site monoheterocylic and even acyclic isoforms (B-GCG, B-GGS and B-GGG) could be readily detected and purified, the A-site monoheterocyclic mutant (A-GGC) yielded no detectable material in several *in vivo* attempts and had to be obtained by *in vitro* post-translational modification. These results are consistent with the A-site heterocycles forming early in a propeptide-directed heterocyclization process, and stabilizing the glycine-rich McbA polypeptide (presumably a random coil) against proteolysis in the microcin-producing *E. coli* cell. The A-site 4,2-fused oxazole–thiazole might fulfill this role by radically

altering the connectivity (and conformation) of the peptide backbone. The B-site tandem heterocycles subsequently formed could be major determinants for DNA recognition, as has been observed for the bisthiazole moiety in bleomycin. Consistent with this model, mutants containing an intact B-site bisheterocycle (B-GCC, B-GSS and B-GSC) have higher antibiotic activity than the corresponding single-ring deletions (B-GCG and B-GGS), and the B-site knockout (B-GGG) is completely inactive. As yet unexplored is the antibiotic activity of MccB17 isoforms lacking one or more of the isolated thiazole and oxazole rings present in the mature antibiotic.

The highest bioactivity was observed with Δ^{+1} and Δ^{0} isoforms of wild-type MccB17 itself, suggesting that the pair of bisheterocycles in this native antibiotic (derived from A-GSC and B-GCS) have been optimized by natural selection. The low abundance of the nine-ring Δ^{+1} MccB17 derivative relative to the native eight-ring Δ^{0} species contrasts with the measurably higher potency of the former. This observation, however, might reveal a strategy adopted by producing cells to maintain their selection advantage in stationary phase. Self-immunity in MccB17-producing cells is afforded by a combination of the dedicated microcin transporter comprising the McbE and McbF proteins, which pump the antibiotic out of the cell, and McbG, which confers protection against endogenous microcin [8]. Cell survival depends on a balance being maintained between the levels and intrinsic activity of endogenous microcins and the protection capacity of the immunity proteins. The production of a predominantly Δ^{+1} isoform appears to have been selected against, perhaps to avoid overwhelming the self-immunity mechanism. The combined bacteriocidal properties of the eight-ring MccB17 and the partially cyclized (five–seven-ring) intermediates is still sufficient to confer a selection advantage to the producing cells in stationary phase.

MccB17 is imported into *E. coli* by an outer membrane porin (OmpF) and the inner membrane receptor SbmA [33]. As indicated by the permeabilized-cell thymidine incorporation assay, the low antibiotic efficacies of the MccB17 analogs are not due to discrimination by OmpF and/or SbmA against these mutants. The low efficacy must be due to a disruption in the recognition of intracellular targets (for example the complex of DNA with DNA gyrase). Given that microcin-induced inhibition of DNA synthesis is the progenitor of a cascade of events that eventually leads to cell death, the differing fates of cells exposed to the various B-site mutants (Figure 11) emphasizes the importance of the B-site bisheterocycle in determining the antibiotic activity of MccB17.

The set of MccB17 analogs described herein, containing mutations at the tandem bisheterocyclic pair of sites, obtained by fermentation in multi-milligram quantities, and spanning a wide range of bioactivities, should be useful for further definition of the molecular determinants of microcin activity. Future objectives include the fine-tuning of tandem 4,2-bisheterocycles as pharmacophores and an extension of the degree to which these moieties can be utilized as independently portable elements of a bioactive compound. In addition, this collection of MccB17 mutants may constitute a useful reagent set to further delineate the nature of the target in the bacterial cell. In this work, we have revalidated earlier reports that the *E. coli* strain bearing the Arg751→Trp mutation in GyrB is resistant to wild-type MccB17 (and have extended this observation to all the mutant microcins as well) increasing the likelihood that this enzyme, a known killing target of the quinolone antibacterial drugs, is at least one of the targets of the antibiotic. Understanding the minimal content and placement of heterocycles in MccB17 for gyrase–DNA complex directed targeting may be enabled by extending this collection of microcin analogs of varying affinity and avidity.

Significance

The *E. coli* peptide antibiotic microcin B17 kills sensitive *E. coli* cells by accumulation of double-strand DNA breaks. DNA gyrase, also the target of the widely used antibacterial quinolone drugs, is one of the killing targets. The two pairs of tandem, fused 4,2-bisheterocycles in MccB17, arising from cyclization of internal Gly–Ser–Cys and Gly–Cys–Ser tripeptide sequences at the A-site and B-site, respectively, have been presumed to function as DNA-targeting elements, given the precedent for intercalation of the comparable 4,2-bisthiazole moiety of bleomycin into double-stranded target DNA. We have addressed the effects of heterocyclic ring number, location and identity on microcin activity in whole cell assays, and compared the antibiotic potency of A-site and B-site MccB17 mutants in a DNA replication assay with toluene-permeabilized cells. *In vivo* production on high-copy plasmids allowed purification of sufficient quantities of wild-type and mutant MccB17 molecules to provide a collection of antibiotic molecules with six–nine rings in wild-type and five–nine rings in mutant isoforms. Analysis of these microcins established that the B-site tandem heterocylic pair was more important for potency than the A-site pair. This initial structure–function analysis will guide future choice of 4,2-bisheterocycles as potential DNA-directing and RNA-directing pharmacophores in combinatorial library strategies.

Materials and methods

Plasmids and strains

Plasmids, pUC19–*mccB17*, (which encodes the *mccB17* operon in the high copy pUC19 vector) and plasmid pET15b(+)His_6-McbA, which encodes an amino-terminal His_6 fusion of the McbA polypeptide under control of the T7 promoter, have been described earlier [5,15]. MccB17-sensitive *E. coli* strain ZK4 (MC4100recA56) [6], the resistant strain VM11 [16] and the MccB17-producing strain ZK4(pMM39) [8] have been reported elsewhere. [α-^{32}P]dTTP (10 mCi/ml) was purchased from Amersham.

Generation of mutant microcins

Mutagenesis of the A-site in *mcbA* was performed by SOE–PCR mutagenesis of plasmid pUC19–*mccB17*, using protocols described elsewhere [15]. The 'outer' forward and reverse primer pairs for SOE–PCR mutagenesis were 5′-GCTCGGTACCCGGGGATCCACTTCAGC-3′ and 5′-CACATTTCCATTGTTCCCGGGCATTACTG-3′, respectively. The nested mutagenic primers pairs were: 5′-GGCGGTTGCTGCGGTGGTCAAGG-3′ and 5′-CCACCTTGACCACCGCAGCAACCGCCGCCG-3′ (for A-GCC), 5′-GGCGGCGGTGGCTGCGGTGGTCAAGGT-3′ and 5′-CCACCTTGACCACCGCAGCAACCGCCGCCG-3′ (for A-GGC) and 5′-GGCGGTAGCAGCGGTGGTCAAGG-3′ and 5′-CCACCTTGACCACCGCTGCTACCGCCGCCG-3′ (for A-GSS).

The B-site mutants were constructed by USE mutagenesis using protocols described earlier [10], or by SOE–PCR mutagenesis of plasmid pUC19–*mccB17*. The selection primer for USE mutagenesis (elimination of the *Sph*I site) was 5′-GCACATGATGCATGCAAGCTTGGCGTAATCATGG-3′. The mutagenic primers were 5′-GGTTGCAGC-AACGGTTGTGGTGGTGGAAACGGTGGCAGC-3′ (B-GCG), 5′-GGTTGCAGCAACGGTTGTTGTGGTGGAAACGGTGGCAGC-3′ (B-GCC), and 5′-GTTGCAGCAACGGTAGTAGTGGTGGAAACGGTGGCAGC-3′ (B-GSS). For SOE–PCR mutagenesis at the B-site, the outer primer pair was comprised of 5′-GCTCGGTACCCGGGGATCCACTTCAGC-3′ and 5′-CACATTTCCATTGTTCCCGGGCATTACTG-3′. The nested mutagenic primer pairs were 5′-GCAACGGTAGTTGTGGTGGAAACGGTGGCAGC-3′ and 5′-CCACCGTTTCCACCACAACTACCGTTGCTGCAACC-3′ (B-GSC), 5′-GCAACGGTGGTGGTGGTGGAAACGGTGGCAGC-3′ and 5′-CCACCGTTTCCACCACCACCACCGTTGCTGCAACC-3′ (B-GGG), and 5′-GCAACGGTGGTAGTGGTGGAAACG-3′ and 5′-CCACCGTTTCCACCACTACCACCGTTGCTGCAACC-3′ (B-GGS).

Mutant plasmids were transformed into *E. coli* DH5α. Cultures (75 ml) in LB/ampicillin (250 μg/ml) were grown overnight at 37°C, and used to inoculate 2 l M63/ampicillin (250 μg/ml) minimal media supplemented with glucose. Cultures were grown to stationary phase at 37°C (30 h), and maintained for an additional 5–6 h. The cells were collected by centrifugation and boiled in 150 ml of 100 mM acetic acid, 1 mM EDTA for 15 min. The clarified supernatant containing crude microcin was applied to a Sep-Pak C_{18} cartridge (Waters), which was washed with 50 ml of 12% acetonitrile (CH_3CN) containing 0.1% trifluoroacetic acid (TFA) to remove flavins and other weakly hydrophobic contaminants. The mixture of heterocyclic microcins was subsequently eluted with 50% CH_3CN, 0.1% TFA. Pure Δ^0 (or Δ^{+1}) microcins were obtained by reversed-phas HPLC purification of this lyophilized residue (4–23 mg) redissolved in dimethyl sulfoxide (DMSO) (solvent A = H_2O + 0.1% TFA; B = CH_3CN + 0.1% TFA, 10–23% B over 25 min, t_R = 16–21 min for the various microcin analogs on a Vydac Preparative C_{18} column). Individual HPLC fractions were analyzed by MALDI–TOF MS or ESI–FT MS to determine heterocycle content and purity.

In vitro *synthesis of α-WT and α-GGC*

SOE–PCR mutagenesis of plasmid pET15b(+)His_6-McbA afforded the corresponding A-GCC McbA fusion peptide for *in vitro* heterocyclization. The outer primer pair comprised 5′-CCGCAAGGAATGGTTGCATGCAAGG-3′ and 5′-CTCATGTTTGACAGCTTATCATCG-3′. The nested mutagenic primer pair comprised 5′-GGCGGCGGTGGCTGCGGTGGTCAAGGT-3′ and 5′-CCACCTTGACCACCGCAGCAACCGCCGCCG-3′. The wild-type and mutant His_6–McbA fusion peptides were expressed in *E. coli* BL21(DE3) cells and purified by affinity chromatography on a Ni^{2+} His-bind column (Novagen) using protocols recommended by the manufacturer.

In vitro heterocyclization of the His_6–McbA fusion peptides was accomplished by incubation of the substrates (70 μM) with affinity-purified microcin B17 synthetase (34 μg) in 300 μl of assay buffer (50 mM Tris–HCl, pH 7.5, 100 mM NaCl, 20 mM $MgCl_2$, 10 mM dithiothreitol (DTT), 2 mM ATP) at 37°C for 25 h. The lyophilized samples of heterocyclized His_6–McbA or the α-GGC mutant were resuspended in 100 μl of 50 mM Tris, pH 8.3, 1 mM EDTA. α-Chymotrypsin was added from a 76 μM stock solution in the same buffer, and the digestion was quenched after 2–3 h at 25°C by freezing (−80°C) or injection onto a C_{18} reversed-phase column. A linear gradient of 10–30% CH_3CN over 40 min was applied, and the various microcin isoforms eluted from 13–22 min, with increased ring content resulting in longer retention times. Completely processed isoforms of each microcin (seven-ring α-GGC and eight-ring α-WT) eluted at ~20 min, and their identities were confirmed by MALDI–TOF MS analysis (α-WT: M_{obs} = 3150.60 Da, M_{calc} = 3150.10 Da; α-GGC: M_{obs} = 3141.40 Da, M_{calc} = 3140.00 Da).

Mass spectrometric analyses

Aliquots (~100 μl) of fractions obtained during the HPLC purification of the microcins were lyophilized and the residue was dissolved in 10 μl of 50% CH_3CN for MALDI–TOF MS analysis. The sample (1 μl) was spotted on a metal target, and mass spectra were acquired in reflectron mode on a Perseptive Biosystems Bioreflex DE STR MALDI–TOF [34] spectrometer using delayed extraction. Alternatively, the lyophilized residue was redissolved in 78:20:2 CH_3CN:water:acetic acid for ESI–FT MS [35] which was performed using either a 4.7 Tesla instrument at Bruker Daltonics (Billerica, MA) or a 9.4 Tesla instrument maintained at the National High-Field FT–ICR User Facility [36]. Spectra were analyzed using GRAMMS-386 (MALDI–TOF), XMASS (4.7 T ESI–FT MS), or Odyssey (9.4 T ESI–FT MS) software and theoretical isotopic distributions were generated using XMASS software (Bruker) or Isopro v.3.0 [37].

For MS/MS analyses, samples were acidified with 2% acetic acid. The multiply-charged ions generated by ESI were analyzed using either a 4.7 or a 9.4 Tesla [36] Fourier-transform mass spectrometer. Briefly, electrosprayed ions produced from either a nanospray emitter (2–4 μm orifice, flow rate ~25–50 nl/min) [38] or a pumped flow apparatus (50 μm orifice, flow rate 400 nl/min) were sampled through an inlet and guided by ion lenses through several stages of differential pumping into the bore of a superconducting magnet (~10^{-9} Torr), wherein ions were trapped. The desired ions were isolated and fragmented by collisions with pulsed Argon gas (~10^{-6} Torr) [24] or with infrared photons [39]. Following such dissociation, the fragment ions were excited and detected. The relative molecular weight values reported here correspond to the neutral monoisotopic peak. Spectra were calibrated externally using bovine ubiquitin (8559.62 Da). Two general types of ions are produced in the MS/MS of polypeptides, containing either the amino or carboxyl terminus and labeled as b-type or y-type ions, respectively [25]. Peak annotation indicates the number of heterocycles formed in a particular fragment ion. For example, ^{7}y25 denotes the ion corresponding to the carboxyl-terminal 25 residues with seven rings formed (140.21 Da lower M_r than that predicted from the DNA-derived sequence).

Determination of microcin concentration

Stock solutions of pure microcin (0.4–1.4 mg) were made up in 50% CH_3CN (80–280 μl), and filtered. A 2 μl aliquot was diluted with 150 μl 50% CH_3CN and the absorbance at 254 nm was measured in a microcuvette. The absorbance of the stock solution was calculated from this measurement, and microcin concentration was expressed in NAU as described in the Results section. Quantitative amino acid analysis of the microcin stocks subsequently enabled antibiotic concentration to be expressed in micromoles, which can be correlated to the NAU values as summarized in Table 1.

Bioassay for microcin activity

Microcin activity was measured using a modified bioassay developed by Yorgey [27]. The microcin-sensitive *E. coli* strain ZK4 and the resistant strain VM11 were used as indicator strains. Lawns of cells were prepared by spreading ~3×10^6 cells (100 μl of a 1 ml LB culture grown at 37°C for 5 h, mixed with 1.5 ml LB and 1.5 ml 0.8% top agar) on LB plates. Aliquots of stock solutions containing defined amounts of microcin (0–1.6 μg) were lyophilized, and the residues were redissolved in 2 μl of DMSO, which were spotted on the lawns. Microcin concentrations in these aliquots ranged from 0–250 μM. The plates were incubated at 37°C for 12 h and halos (zones) of growth inhibition were quantified from imaged plates by densitometric analysis using NIH Image v.1.61. Halo intensities were normalized against the plate background to compensate for varying exposures in the filming

process. This process proved more accurate than the default practice of measuring halo diameters, especially when the low activity of certain microcin analogs resulted in weak halos due to partial growth inhibition.

Assay for replicative DNA synthesis

Toluene-permeabilized *E. coli* ZK4 cells were prepared as described elsewhere [30] and stored at −80°C. Appropriate aliquots of stock solutions of the various Δ^0 MccB17 analogs (in 50% CH_3CN) were lyophilized and redissolved in 5 µl of DMSO, 24 µl of DNA synthesis buffer (230 mM Tris HCl pH 7.5, 22 mM $MgCl_2$, 714 mM KCl, 4 mM ATP, 0.955 mM β-mercaptoethanol, and 200 µM each dNTP), and 79 µl H_2O. The assay mixture was incubated at 30°C for 5 min after the addition of 17 µl of toluene-treated ZK4 cells. [α-^{32}P]dTTP was subsequently added (0.12 µCi), and the assay temperature was maintained at 30°C. Aliquots (20 µl) were withdrawn at appropriate time points and quenched with 200 µl of cold 10% TCA solution. Aliquots (160 µl) of the acid quenches were loaded on a glass fiber filter using a 48-well slot-blot apparatus (Biorad). The filter was washed with cold 0.01 N HCl (10 × 200 µl), and precipitated radioactivity was quantified using a phosphorimager.

Acknowledgements

This research was supported by NIH Grant GM 20011 to C.T.W. R.S.R. is a Parke-Davis Fellow of the Life Sciences Research Foundation. N.L.K. is an NIH postdoctoral fellow (F32 AI 10087-02). J.C.M. is an American Cancer Society Postdoctoral Research Fellow (PF4332). We thank Frank Laukien, Gary Kruppa and Paul Speir of Bruker Daltonics for access to their FTMS instrument and for assistance with data collection. We also thank Alan Marshall for granting access to the 9.4 Tesla ESI–FTMS mass spectrometer (National High-Field FT–ICR MS Facility, NHMFL, NSF CHE-94-13008), and Roberto Kolter for helpful discussions and critical reading of the manuscript.

References

1. San Millán, J.L., Kolter, R. & Moreno, F. (1985). Cloning and mapping of the genetic determinants of microcin-B17 production and immunity. *J. Bacteriol.* **163**, 275-281.
2. San Millán, J.L., Kolter, R. & Moreno, F. (1985). Plasmid genes required for microcin B-17 production. *J. Bacteriol.* **163**, 1016-1020.
3. Davagnino, J., Herrero, M., Furlong, D., Moreno, F. & Kolter, R. (1986). The DNA replication inhibitor microcin B17 is a forty-three-amino-acid protein containing sixty percent glycine. *Proteins* **1**, 230-238.
4. Yorgey, P., Davagnino, J. & Kolter, R. (1993). The maturation pathway of microcin B17, a peptide inhibitor of DNA gyrase. *Mol. Microbiol.* **9**, 897-905.
5. Li, Y.-M., Milne, J.C., Madison, L.L., Kolter, R. & Walsh, C.T. (1996). From peptide precursors to oxazole and thiazole-containing peptide antibiotics. *Science* **274**, 1188-1193.
6. Yorgey, P., *et al.* & Kolter, R. (1994). Posttranslational modifications in microcin B17 define an additional class of DNA gyrase inhibitor. *Proc. Natl Acad. Sci. USA* **91**, 4519-4523.
7. Bayer, A., Freund, S. & Jung, G. (1995). Post-translational heterocyclic backbone modifications in the 43-peptide antibiotic microcin B17. Structure elucidation and NMR study of a ^{13}C, ^{15}N-labelled gyrase inhibitor. *Eur. J. Biochem.* **234**, 414-426.
8. Garrido, M.C., Herrero, M., Kolter, R. & Moreno, F. (1988). The export of the DNA replication inhibitor microcin B17 provides immunity for the host cell. *EMBO J.* **7**, 1853-1862.
9. Herrero, M. & Moreno, F. (1986). Microcin B17 bocks DNA replication and induces the SOS system in *Escherichia coli*. *J. Gen. Microbiol.* **132**, 393-402.
10. Sinha Roy, R., Belshaw, P.J. & Walsh, C.T. (1998). Mutational analysis of post-translational heterocycle biosynthesis in the gyrase inhibitor microcin B17: distance dependence from propeptide and tolerance for substitution in a GSCG cyclizable sequence. *Biochemistry* **37**, 4125-4136.
11. Sinha Roy, R., Kim, S., Baleja, J.D. & Walsh, C.T. (1998). Role of the microcin B17 propeptide in substrate recognition: solution structure and mutational analysis of $McbA_{1-26}$. *Chem. Biol.* **5**, 217-228.
12. Madison, L.L., Vivas, I.E., Li, Y.-M., Walsh, C.T. & Kolter, R. (1997). The leader peptide is essential for the post-translational modification of the DNA gyrase inhibitor microcin B17. *Mol. Microbiol.* **23**, 161-168.
13. Belshaw, P.J., Sinha Roy, R., Kelleher, N.L. & Walsh, C.T. (1998). Kinetics and regioselectivity of peptide-to-heterocycle conversions by microcin B17 synthetase. *Chem. Biol.* **5**, 373-384.
14. Kelleher, N.L., Belshaw, P.J. & Walsh, C.T. (1998). Regioselectivity and chemoselectivity analysis of oxazole and thiazole ring formation by the peptide-heterocyclizing microcin B17 synthetase using high-resolution MS/MS. *J. Am. Chem. Soc.* **120**, 9716-9717.
15. Milne, J.C., Eliot, A.C., Kelleher, N.L. & Walsh, C.T. (1998). ATP/GTP hydrolysis is required for oxazole and thiazole biosynthesis in the peptide antibiotic microcin B17. *Biochemistry* **37**, 13250-13261.
16. Vizán, J.L., Hernández-Chico, C., del Castillo, I. & Moreno, F. (1991). The peptide antibiotic microcin B17 induces double-stranded cleavage of DNA mediated by *E. Coli.* DNA gyrase. *EMBO J.* **10**, 467-476.
17. Gellert, M., Mizuuchi, K., O'Dea, M.H. & Nash, H.A. (1976). DNA gyrase: an enzyme that introduces superhelical turns into DNA. *Proc. Natl Acad. Sci. USA* **73**, 3872-3876.
18. Shen, L.L. & Chu, D.T.W. (1996). Type II DNA topoisomerases as antibacterial targets. *Curr Pharm Des* **2**, 195-208.
19. Vanderwall, D.E., Lui, S.M., Wu, W., Turner, C.J., Kozarich, J.W. & Stubbe, J. (1997). A model of the structure of HOO-Co.bleomycin bound to d(CCAGTACTGG): recognition at the d(GpT) site and implications for double-stranded DNA cleavage. *Chem. Biol.* **4**, 373-387.
20. Zuber, G., Quada Jr., J.C. & Hecht, S.M. (1998). Sequence selective cleavage of a DNA octanucleotide by chlorinated bithiazoles and bleomycins. *J. Am. Chem. Soc.* **120**, 9368-9369.
21. Ho, S.N., Hunt, H.D., Horton, R.M., Pullen, J.K. & Pease, L.R. (1989). Site-directed mutagenesis by overlap extension using the polymerase chain reaction. *Gene* **77**, 51-59.
22. Deng, W.P. & Nickoloff, J.A. (1992). Site-directed mutagenesis of virtually any plasmid by eliminating a unique site. *Anal. Biochem.* **200**, 81-88.
23. Genilloud, O., Moreno, F. & Kolter, R. (1989). DNA sequence, products, and transcriptional pattern of the genes involved in production of the DNA replication inhibitor microcin B17. *J. Bacteriol.* **171**, 1126-1135.
24. Gauthier, J.W., Trautman, T.R. & Jacobson, D.B. (1991). Sustained off-resonance irradiation for collision-activated dissociation involving Fourier-transform mass-spectrometry – collision-activated dissociation technique that emulates infrared multiphoton dissociation. *Anal. Chim. Acta* **246**, 211-225.
25. Roepstorff, P. & Fohlman, J. (1984). Proposal for a common nomenclature for sequence ions in mass spectra of peptides. *Biomed. Mass. Spec.* **11**, 601.
26. Mayr-Harting, A., Hedges, A.J. & Berkeley, R.C.W. (1972). Methods for studying bacteriocins. *Meth. Microbiol.* **7A**, 315-422.
27. Yorgey, P.S. (1993). The structure and biosynthesis of microcin B17, a novel DNA gyrase inhibitor. Ph.D. Thesis, Harvard University, Cambridge.
28. Takita, T., Muraoka, Y., Nakatani, T., Fujii, A., Umezawa, Y. & Naganawa, H. (1978). Chemistry of bleomycin XIX. Revised structures of bleomycin and phleomycin. *J. Antibiot.* **31**, 801-804.
29. Ichiba, T., Yoshida, W.Y., Scheuer, P.J., Higa, T. & Gravalos, D.G. (1991). Hennoxazoles: bioactive bisoxazoles from a marine sponge. *J. Am. Chem. Soc.* **113**, 3173-3174.
30. Moses, R.E. (1972). Relicative deoxyribonucleic acid synthesis in a system diffusable for macromolecules. *J. Biol. Chem.* **247**, 6031-6038.
31. Selva, E., Montanini, N., Stella, S., Soffientini, A., Gastaldo, L. & Denaro, M. (1997). Targeted screening for elongation factor Tu binding antibiotics. *The J. Antibiot.* **50**, 22-26.
32. Asencio, C., Pérez-Díaz, J.C., Martínez, M.C. & Baquero, F. (1976). A new family of low molecular weight antibiotics from enterobacteria. *Biochem. Biophys. Res. Commun.* **69**, 7-14.
33. Lavina, M., Pugsley, A.P. & Moreno, F. (1986). Identification, mapping, cloning and characterization of a gene (*sbmA*) required for microcin B17 action on Escherichia coli K12. *J. Gen. Microbiol.* **132**, 1685-1693.
34. Hillenkamp, F., Karas, M., Beavis, R.C. & Chait, B.T. (1991). Matrix-assisted laser desorption ionization mass-spectrometry of biopolymers. *Anal. Chem.* **63**, 1193A-1203A.
35. Fenn, J.B., Mann, M., Meng, C.K. & Wong, S.F. (1990). Electrospray ionization - principles and practice. *Biol. Mass Spectrom.* **9**, 37-70.
36. Senko, M.W., *et al.* & Marshall, A.G. (1996). Electrospray-ionization Fourier-transform ion-cyclotron resonance at 9.4 T. *Rapid Commun. Mass Spectrom.* **10**, 1824-1828.
37. Senko, M.W., Beu, S.C. & McLafferty, F.W. (1995). Determination of monoisotopic masses and ion populations for large biomolecules from resolved isotopic distributions. *J. Am. Soc. Mass. Spectrom.* **6**, 229-233.
38. Wilm, M. & Mann, M. (1996). Analytical properties of the nanoelectrospray ion-source. *Anal. Chem.* **68**, 1-8.
39. Little, D.P., Speir, J.P., Senko, M.W., O'Connor, P.B. & McLafferty, F.W. (1994). Infrared multiphoton dissociation of large multiply-charged ions for biomolecule sequencing. *Anal. Chem.* **66**, 2809-2815.